RSC Advances




ROYAL SOCIETY OF CHEMISTRY

www.rsc.org/advances

# Self-assembly of alkyldithiols on a novel dendritic silver nanostructure electrodeposited on a stainless steel wire as a fiber coating for solid-phase microextraction

Yaoxia Yang [a,c], Mei Guo [a], Yida Zhang [a], Wenlan Song [a], Yi Li [a], Xuemei Wang [a,b], Xinzhen Du [a,b*]

[a] College of Chemistry and Chemical Engineering, Northwest Normal University, Lanzhou 730070, China

[b] Key Laboratory of Bioelectrochemistry & Environmental Analysis of Gansu, Lanzhou 730070, China

[c] Key Laboratory of Polymer Materials of Gansu Province, Lanzhou 730070, China

**Abstract:**

A facile and efficient electrodeposition approach for the controllable preparation of dendritic silver nanostructure was developed on an etched stainless steel (ESS) wire. Subsequently, self-assembled of alkyldithiols (HS-$C_x$-SH, x=2, 3, 6, 8) was performed on the dendritic Ag coating via Ag-S bonding. The octanedithiol modified Ag nanodendrites (AgNDs) coated ESS fiber (HS-$C_8$-S-AgNDs/ESS) was then assessed for SPME of polycyclic aromatic

* Corresponding author. Tel.: +86 931 7970796; fax: +86 931 7970796
*E-mail address:* duxz@nwnu.edu.cn (X.-Z. Du).

hydrocarbons (PAHs), ultraviolet (UV) filters, polychlorinated biphenyls (PCBs), chlorophenols (CPs), phthalate esters (PAEs) and substituted anilines coupled to high-performance liquid chromatography with UV detection (HPLC-UV). This fiber exhibits higher extraction capability and good selectivity for PAHs, UV filters, PCBs and Triclosan compared to CPs, PAEs and substituted anilines. In particular, the microextraction conditions were investigated and optimized for SPME performance of UV filters. Under the optimized conditions, the developed method showed good linearity between 0.30 and 400 μg $L^{-1}$ with corresponding correlation coefficients in the range of 0.9973-0.9986. The limits of detection ranged from 0.05 to 0.12 μg $L^{-1}$. The relative standard deviation for fiber-to-fiber reproducibility of five fabricated fibers in the same batch was less than 8.2%. The expanded uncertainties were below 6.9 % (coverage factor k=2). The developed method was practically applied to the preconcentration and determination of trace UV filters from real environmental water samples.

***Keywords*:** Silver nanodendrites; Self-assembly; Solid-phase microextraction; High-performance liquid chromatography; Ultraviolet filters

## 1. Introduction

Nowadays nanotechnology is one of the most important trends in material science. Due to ultra-small size, nanomaterials possess unique physical and chemical properties.[1] Therefore

their design, synthesis, characterization and applications are critical aspects for the emerging field of nanomaterials. It was expected that the large specific surface area of nanomaterials can improve the detection sensitivity and miniaturize the devices. Thus sample separation and preconcentration techniques based on nanomaterials have played important roles in many analytical procedures. Moreover nanomaterials can also be functionalized with different chemical groups to enhance their affinity toward specified analytes, which tailors their selectivity for the extraction of target analytes in complex matrices such as environmental and biological samples.[2]

Solid-phase microextraction (SPME) is a universal, convenient and solvent-free sample preparation technique. It was firstly introduced by Pawliszyn in 1990s[3] and has gained its popularity in the analyses of environmental,[4] food,[5,6] pharmaceutical[7] and biological[8] samples. SPME is an extraction technique based on the partitioning of the organic analytes between the sample matrix and the extraction coating, which is typically immobilized on a fused silica fiber or metal wire. Therefore the fiber coating material is critical in improving the SPME performance. Recently, gold (Au) or silver (Ag) nanoparticles were fabricated as fiber coatings for SPME of specified analytes.[9,10] Organic molecules containing thiol group (-SH) can be chemically bonded onto the surface of Au or Ag to form a self-assembled monolayer (SAM).[11] This approach has been employed to develop novel Au and Ag supported fibers[12-14] and modify Au nanoparticles coatings,[15,16] which were successfully applied in SPME.

Nanodendrites are a promising class of materials that are highly attractive due to their high surface area-to-volume ratio, high porosity, high degree of connectivity and a large number of edges and corner atoms.[17] These characteristics make the nanodendrites highly useful for a variety of applications including catalysis,[18] chemical sensing[19-21] and surface enhanced Raman scattering.[22-25] In particular, considerable efforts have been focused on the design, synthesis and application of Au nanodendrites based on different advanced strategies.[26-33] Less attention has been paid to Ag nanodendrites (AgNDs) and subsequent surface modification and application in SPME.

In this work, we described a new approach to rapid and controllable electrodeposition of Ag nanodendritic coating on the surface of the etched stainless steel (ESS) wire using cyclic voltammetry (CV) followed by self-assembly of alkyldithiols (HS-$C_x$-SH, x=2, 3, 6, 8) occurring uniquely on Ag coating. The silver layer greatly increases the surface area of stainless steel (SS) wire and serves as a supporting substrate for subsequent organic funtionalization via the Ag-S bond. Surface morphology and elemental composition of the prepared HS-$C_8$-S-AgNDs coated SPME fiber were investigated by scanning electron microscope and energy dispersive X-ray spectroscopy. Their extraction performance was evaluated for the concentration and separation of six organic compounds coupled to high-performance liquid chromatography with UV detection (HPLC-UV). In particular, the extraction conditions were investigated and optimized for the concentration and

determination of UV filters with 1,8-octanedithiol (HS-$C_8$-SH) modified AgNDs coated ESS fiber (SH-$C_8$-S-AgNDs/ESS). Meanwhile, we also estimated the uncertainty and calculate expanded uncertainty on account of uncertainty is always present at every step of a procedure.[34-37] The SPME-HPLC-UV procedure was established to preconcentrate and determine UV filters from real environmental water. Furthermore the SPME performance of the HS-$C_8$-S-AgNDs/ESS fiber was compared with that of commercial polyacrylate (PA) and polydimethylsiloxane (PDMS) fibers under the optimized conditions.

## 2. Experimental

### 2.1. Materials and reagents

The stainless steel wire (80 mm, 0.25 mm O.D.) was supplied by Gaoge (Shanghai, China). Hydrofluoric acid (40%) was purchased from Shuangshuang Chemicals Co., Ltd, (Yantai, China). Silver nitrate ($AgNO_3$) was purchased from Baiyin Chemical Reagents Company (Baiyin, China). Sodium chloride (NaCl) was purchased from Sinopharm Chemical Reagent Co., Ltd. (Shanghai, China). HPLC-grade methanol was purchased from Yuwang Chemical Company (Yucheng, China). 1,2-Ethylenedithiol (HS-$C_2$-SH), 1,3-propanedithiol (HS-$C_3$-SH) and 1,6-hexanedithiol (HS-$C_6$-SH) was purchased from Sahn Chemical technology Co., Ltd. (Shanghai, China). 1,8-Octanedithiol (HS-$C_8$-SH) was purchased from Acros (Geel, Belglum, NJ, USA). Certified of 2-hydroxy-4-methoxybenzophenone (BP-3), 2-ethylhexyl 4-(*N,N*-

dimethylamino) benzoate (OD-PABA), 2-ethylhexyl 4-methoxycinnamate (EHMC), dimethyl phthalate (DMP), diethyl phthalate (DEP), di-*n*-butyl phthalate (DBP), di-*n*-octyl phthalate (DOP), di-(2-ethylhexyl) phthalate (DEHP), 2-chlorophenol (2-CP), 2,4-dichlorophenol (2,4-CP), 2-(2,4-dichlorophenoxy)-5-chlorophenol (Triclosan), 2,4',5-trichlorobiphenyl (PCB 31), 2,4,4'-trichlorobiphenyl (PCB 28), 2,3',4,4',5-pentachlorobiphenyl (PCB 118), 2,2',4,4',5,5'-hexachlorobiphenyl (PCB 153), aniline, 4-nitroaniline and benzidine were purchased from AccuStandard (New Haven, CT, USA). Certified 2-ethylhexyl salicylate (EHS) was purchased from Dr. Ehrenstorfer GmbH (Augsburg, Germany). Certified naphthalene (Nap), phenanthrene (Phe), anthracene (Ant), fluoranthene (Fla) and 4-methylaniline were purchased from Aldrich (St. Louis, MO, USA). Individual standard stock solutions were prepared in methanol at a concentration of 1 g $L^{-1}$ for substituted anilines and CPs as well as 100 mg $L^{-1}$ for PAHs, UV filters, PCBs and PAEs, resectively, storing at 4 $^{o}$C in the refrigerator. A polyacrylate (PA, 85μm thickness) and polydimethylsiloxane (PDMS, 100 μm thickness) fibers were obtained from Supelco (Bellefonte, PA, USA). All chemicals were analytical reagents.

**2.2. Apparatus**

All chromatographic separation was performed with isocratic elution on a Waters 600E multi-solvent delivery system (HPLC, Milford, MA, USA) equipped with a Waters 2487 dual λ absorbance detector and a Zorbax Eclipse Plus $C_{18}$ column (150 mm×4.6 mm, 5 μm,

Agilent, USA). Data was collected with a N2000 workstation (Zhejiang University, China). A SPME device was modified from a commercially available 2-μL HPLC microsyringe (Gaoge, Shanghai, China). The desorption procedure was carried out in SPME-HPLC interface (Supelco, PA, USA). The proposed fiber was characterized by an Ultra Plus scanning electron microscope (SEM, Zeiss, Oberkochen, Germany) equipped with semi-quantitative microanalysis by Aztec-X-80 energy dispersive X-ray spectroscopy (EDS, Oxford, UK). The electrodeposition procedure was performed on a CHI832D electrochemical analyzer (Chenhua, Shanghai, China). The extraction procedure was performed in a DF-101S thermostated water bath with a magnetic stirrer (Zhengzhou, China). Ultrapure water was obtained from a Sudreli SDLA-B-X water purification system (Chongqing, China).

**2.3. Fabrication of HS-$C_x$-S-AgNDs/ESS fiber**

One end of the stainless steel (SS) wire was firstly washed in acetone for 10 min in an ultrasonic bath to remove the organic pollutants and then rinsed with ultrapure water for 10 min. Subsequently the SS wire was etched for 60 min at 40□ in hydrofluoric acid (40%) according to improved procedure.[38] Afterwards the ESS fiber was washed with ultrapure water thoroughly and dried at nitrogen atmosphere.

The electrodeposition of AgNDs coating onto the surface of ESS wire was performed by cyclic voltammetry (CV) in electrolytic solution of $AgNO_3$ (0.01 mol $L^{-1}$) with three electrode system using the ESS wire as a working electrode, a Pt rod as a counter electrode

and a saturated calomel electrode as a reference electrode. The potential was applied from -0.3 V to 0.3 V for 20 CV cycles at a scan rate of 20 mV $s^{-1}$. Thereafter the fabricated AgNDs/ESS fiber was rinsed with water and ultrasonically cleaned in ethanol for 0.5 min. The AgNDs/ESS fiber was directly dipped into ethanol solution containing alkyldithiols of 0.1%(w/w) for 24 h at room temperature. After self-assembly, the HS-$C_x$-S-AgNDs/ESS (x=2, 3, 6, 8) fibers were washed with ethanol to removed excess alkyldithiols and dried in nitrogen atmosphere.

**2.4. SPME-HPLC procedure**

The extraction procedure was performed with 15 mL of working standard solution or sample solution in a 20-mL glass vial with magnetic stirrer bar. The HS-$C_x$-S-AgNDs/ESS fiber was immersed into the stirred and heated sample solution for extraction. After SPME, the fiber was retracted from the sample solution and immediately introduced into the SPME-HPLC interface for static desorption in mobile phase and chromatographic analysis. Methanol/water of 88/12 (v/v), 86/14 (v/v), 90/10 (v/v), 70/30 (v/v), 75/25 (v/v), and 60/40 (v/v) was used as mobile phases at a flow rate of 1 mL $min^{-1}$ for HPLC analysis of PAHs, UV filters, PCBs, CPs, PAEs and substituted anilines, respectively. 254 nm, 310 nm, 254 nm, 282 nm, 280 nm and 280 nm were employed for corresponding UV detection. Prior to next extraction, the proposed fiber was cleaned in methanol for 15 min and ultrapure water for 10

min to eliminate carry over between samples. All the experiments were performed in triplicate, otherwise stated.

**2.5. Real water samples**

Real environment water samples include 4 river water, 1 wstewater and 1 snow water samples. River water samples were freshly collected from different sites in the Lanzhou section of the Yellow River. A wastewater sample was collected from local wastewater treatment plant and the snow water sample was collected from Yantan area of Lanzhou. All samples were filtered through 0.45 μm micropore membranes and then stored in amber glass containers in fridge at 4□. Fig. 1 illustrates a flow diagram of the method used for the concentration and determination of UV filters in water samples by SPME-HPLC-UV.

**Fig. 1**

**Fig. 1.** Flow diagram of the procedure of UV-filters determination in water samples by HPLC-UV method.

**3. Results and discussion**

**3.1. Electrochemical fabrication of AgNDs/ESS fiber**

Pretreatment of the SS wire can ensure the firmness and uniformity of the fiber coatings before chemical deposition,[9] hydrothermal growth[39] or dipping coating.[40] The etching step

offers very rough surface for the SS wire, enhances the binding strength between the fiber coating and the porous ESS substrate. CV allows to precisely control the uniformity and the deposition rate for subsequent electrochemical fabrication of nanostructured coatings for excellent extraction. As compared with that of bare SS wire shown in Fig. 2a, the ESS wire exhibits very rough and porous surface structure (Fig. 2b). The etching step provides an ideal supporting substrate for subsequent electrodeposition of AgNDs coating. It can be clearly seen from Fig. 2c that the AgNDs coating is immobilized onto the surface of the ESS wire.

**Fig. 2**

**Fig. 2.** SEM images of bare SS wire (a×10000), ESS wire (b×10000), AgNDs coating (c×20000) and SH-$C_8$-S-AgNDs/ESS (d×20000) fibers. Conditions: applied voltage, -0.3 V to 0.3 V; scan rate, 20 mV $s^{-1}$; CV cycles, 20; SAM,12 h; 25□.

### 3.2. Self-assembly of alkyldithiols on AgNDs coating

Self-assembly of different alkyldithiols 0.1%(w/w) was performed on the AgNDs coating in 5 mL ethanol solution containing via Ag-S bonding. Fig. S1 shows the surface morphology of different alkyldithiols modified AgNDs/ESS fibers (HS-$C_x$-S-AgNDs/ESS, x=2, 3, 6, 8). More compact surface structures were achieved compared to that of AgNDs coating (Fig. 2d). Fig. 2d shows the SEM image of the HS-$C_8$-AgNDs/ESS fiber. Moreover larger Ag particles

were observed after self-assembly for a longer time (Fig. S2). Such surface morphology implies that self-assembly of alkyldithiol molecules was formed on the AgNDs coating. Meanwhile corresponding extraction performance of different HS-$C_x$-S-AgNDs/ESS fibers in the same batch was compared in Fig. 3 using UV filters as model compounds. The HS-$C_8$-AgNDs/ESS fiber gives the best extraction efficiency for UV filters (OD-PABA, EHMC and EHS). This result suggests that self-assembly of different alkyldithiols on the AgNDs coating result in the formation of the organic-inorganic hybrid coating and greatly modifies surface properties of the AgNDs/ESS fiber. In the following experiment, the HS-$C_8$-S-AgNDs/ESS fiber was employed for further study.

**Fig. 3**

**Fig. 3.** Chromatograms of UV filters by SPME-HPLC with the SH-$C_2$-S-AgNDs/ESS (a), SH-$C_3$-S-AgNDs/ESS (b), SH-$C_6$-S-AgNDs/ESS (c) and SH-$C_8$-S-AgNDs/ESS (d) fibers. Conditions: UV filters, 100 μg $L^{-1}$; extraction, 30 min; desorption, 4 min; temperature, 35 $^{o}$C; stirring, 500 r $min^{-1}$.

### 3.3. Surface analysis of the HS-$C_8$-S-AgNDs/ESS fiber

Surface composition of the HS-$C_8$-S-AgNDs/ESS fiber was also comparatively investigated by EDS. As compared with the bare SS wire (Fig. 4a), the ESS wire exhibits

very similar EDS spectra (Fig. 4b), indicating that the etching step can not change the surface composition of the SS wire but greatly modify the surface morphology of the SS wire. After electrodeposition of AgNDs, a strong characteristic signal for Ag was simply observed at 2.98 keV (Fig. 4c). Therefore full coverage of AgNDs was achieved on the surface of the ESS substrate via electrochemical deposition. When 1,8-octanedithiol is chemically bonded onto the surface of AgNDs coating, an enhanced characteristic signal for carbon and corresponding characteristic signal for sulfur also appear in Fig. 4d at the same time. Moreover stronger carbon and sulfur signals as well as weaker Ag signal were observed after self-assembly of 1,8-octanedithiol molecules for a longer time (Fig. S3), indicating that more HS-$C_8$-S- groups were anchored on the surface of AgNDs coating via Ag-S bonding. AgNDs as novel supporting substrate acted as a template for the self-assembly of HS-$C_8$-S- groups. These phenomena provide additional evidence for the results obtained by SEM.

**Fig. 4**

**Fig. 4.** EDS spectra of bare SS wire (a), ESS wire (b), AgNDs/ESS fiber (c) and SH-$C_8$-S-AgNDs/ESS fiber (d).

### 3.4. Extraction efficiency and selectivity

The extraction performance of the prepared fibers was further examined. As compared with the bare SS fiber (Fig. S4b), the ESS fiber exhibits improved extraction efficiency for OD-PABA, EHMC and EHS (Fig. S4c) because the etching step greatly increases the surface area of the SS wire. As shown in Fig. S4d, the AgNDs/ESS fiber shows better extraction efficiency for OD-PABA, EHMC and EHS due to the hydrophobic interaction between the AgNDs coating and UV filters.[10] After self-assembly, the HS-$C_8$-S-AgNDs/ESS fiber exhibits the best extraction efficiency for above UV filters. This result suggests that the self-assembly of HS-$C_8$-S- groups remarkably modify the surface properties of the AgNDs/ESS fiber and enhance the affinity for studied UV filters.

Extraction selectivity of the HS-$C_8$-S-AgNDs/ESS fiber was investigated using PAHs, UV filters, PCBs, CPs, PAEs and substituted anilines as model analytes. As shown in Fig. 5, the HS-$C_8$-S-AgNDs/ESS fiber exhibits better extraction selectivity for PAHs, UV filters (OD-PABA, EHMC and EHS), PCBs and Triclosan. By contrast, this fiber only shows very low extraction capability for BP-3. In the case of CPs (2-CP and 2,4-DCP), PAEs and substituted anilines (not shown), negligible extraction appears. These results clearly demonstrate that the HS-$C_8$-S-AgNDs/ESS fiber has strong interaction toward PAHs, UV filters (with lower solubility), PCBs and Triclosan. Therefore, the fabricated fiber is a good candidate for the preconcentration and separation of trace PAHs, UV filters, PCBs, and Triclosan from water samples. In particular, the HS-$C_8$-S-AgNDs/ESS fiber offers a weakly polar coating surface

due to the presence of $C_8$ chains with thiol groups and exhibits efficient extraction for OD-PABA, EHMC and EHS. Thus this fiber was employed to optimize its extraction performance for OD-PABA, EHMC and EHS in subsequent study.

**Fig. 5**

**Fig. 5.** Typical chromatograms of direct HPLC for PAEs (a), CPs (c), PCBs (e), UV filters (g) and PAHs (i) as well as corresponding SPME-HPLC with SH-$C_8$-S-AgNDs/ESS fiber for PAEs (b), CPs (d), PCBs (f), UV filters (h) and PAHs (j) for water spiked with 100 μg $L^{-1}$ each analyte.

### 3.5. Optimization of SPME

To improve extraction efficiency, the extraction conditions such as extraction time, desorption time, extraction temperature, stirring rate, ionic strength and pH were optimized. The peak areas were used to examine the extraction performance of the proposed HS-$C_8$-S-AgNDs/ESS fiber for OD-PABA, EHMC and EHS in aqueous samples.

#### *3.5.1. Dependence of extraction efficiency on extraction and desorption time*

The extraction time is depends strongly on equilibrium time, which is associated with distribution properties of analytes between the fiber coating and sample solution. The extraction efficiency increases with extraction time and reaches a plateau at constant

temperature. Fig. 6a shows that the extraction equilibrium was reached at about 40 min. Subsequently static solvent desorption of the extracted UV filters was examined in mobile phase, the equilibrium of desorption was achieved within 4 min (Fig. 6b). No carry-over of target UV filters was detected for the second desorption. In the following experiments, 40 min and 4 min were employed for extraction and desorption, respectively.

**Fig. 6**

**Fig. 6.** Dependence of extraction efficiency on extraction time (a), desorption time (b), temperature (c) and stirring rate (d). Error bars are corrected standard deviation of peak areas for three replicates at the 95% confidence level.

***3.5.2. Dependence of extraction efficiency on temperature***

Temperature plays a very important role in SPME based on adsorption mechanism. It not only influences the diffusion coefficients but also affects the distribution constants. Fig. 6c shows the dependence of extraction efficiency of UV filters on temperature from 15 $^{o}$C to 65 $^{o}$C. Heating facilitates the diffusion of analytes in aqueous solution at lower temperature than 35 $^{o}$C and thereby improves extraction efficiency. However, higher temperature than 35 $^{o}$C results in poor extraction of analytes because the surface adsorption is generally an

exothermic process. Moreover higher temperature also increases the solubility of analytes in aqueous phase. Thus 35 $^{o}$C was used in subsequent study.

***3.5.3. Dependence of extraction efficiency on stirring***

Generally stirring is frequently employed to accelerate the mass transfer of analytes from the sample matrix into the fiber coating, allowing for the extraction equilibrium in a shorter time. As a result, the stirring rate was studied from 300 r min$^{-1}$ to 800 r min$^{-1}$. The maximum extraction efficiency was achieved at the stirring rate of 500 r min$^{-1}$ shown in Fig. 6d. Therefore, the stirring rate was fixed at 500 r min$^{-1}$ for SPME.

***3.5.4. Dependence of extraction efficiency on ionic strength***

Addition of inorganic salt is usually used to lower the solubility of organic analytes in the sample matrix due to the salting-out effect and improve their extraction efficiency. Consequently ionic strength was adjusted with different NaCl contents from 0 to 30%(w/w). In the presence of NaCl less than 3%, the extraction efficiency of UV filters was slightly decreased. Thereafter the extraction efficiency was obviously decreased with the increasing concentration of NaCl. In the case of about 5% NaCl, chloride ions may destroy the hydrogen bonding interaction between the thiol groups and UV filters to some extent. In addition, the viscosity of aqueous phase increases in the case of higher NaCl content, which decreases the diffusion coefficients of the analytes in aqueous phase.[41] More negative effect of NaCl on the extraction occurs. As a result, salt was not added in the following study.

### *3.5.5. Dependence of extraction efficiency on pH*

The pH value of sample solution plays a crucial role in the extraction of acidic or basic analytes. Therefore, the dependence of extraction efficiency on pH was studied between 3.0 and 9.0. The extraction efficiency decreased at lower pH due to the protonation of target analytes. Also the protonation of thiol groups could have a negative effect on extraction efficiency to some extent. The best extraction efficiencies were observed at pH 7.0 because the neutral forms of UV filters are favorable for their adsorption onto the HS-$C_8$-S-AgNDs/ESS fiber. At higher pH, however, the extraction efficiency gradually decreased. Therefore, the pH value was fixed at 7.0 for SPME.

## 3.6. Method validation

Under the optimized conditions, the proposed analytical method was investigated by extracting a series of standard water samples ranging from 0.1 to 400 $\mu g \cdot L^{-1}$. Analytical parameters are listed in Table 1. The linearity ranged from 0.30 to 400 $\mu g \cdot L^{-1}$ for OD-PABA and EHMC and from 0.50 to 400 $\mu g \cdot L^{-1}$ for EHS, with all the correlation coefficients being larger than 0.9973. Limits of detection (LOD) and limits of quantification(LOQ) were obtained based on the signal to-noise ratio of 3 and 10, respectively. LODs were in the range 0.05-0.12 $\mu g\ L^{-1}$ and LOQs in the range 0.17-0.40 $\mu g\ L^{-1}$. The precision of the method was tested by performing five consecutive extractions. The single fiber repeatability for five extraction runs of working solution spiked at 100 $\mu g\ L^{-1}$ varied from 4.2% to 6.6% for intra-

day determination and from 5.7% to 7.1% for inter-day determination. The fiber-to-fiber reproducibility was also investigated with five fabricated fibers in the same batch and varied from 6.3% to 8.2%. The expanded uncertainties were below 6.9 % (coverage factor k=2) and the expanded uncertainties of each analyte determined were estimated according the previous study.[35]

**Table 1**

**Table 1** Analytical parameters of the proposed method (n=5)

| Parameter | | Value | | |
|---|---|---|---|---|
| Analyte | | OD-PABA | EHMC | EHS |
| Linear ranges ($\mu g \cdot L^{-1}$) | | 0.30-400 | 0.30-400 | 0.50-400 |
| $r^2$ | | 0.9986 | 0.9979 | 0.9973 |
| Recovery (%) | | 99.5±6.8 | 102.0±6.0 | 97.6±7.3 |
| Expanded uncertainty (%) | | 6.2 | 5.8 | 6.9 |
| Single fiber repeatability | Intra-day (%) | 4.2 | 6.4 | 6.6 |
| | Inter-day (%) | 5.7 | 7.5 | 7.1 |
| Fiber-to-fiber reproducibility (%) | | 6.3 | 8.2 | 7.4 |
| LOD ($\mu g \cdot L^{-1}$) | | 0.05 | 0.07 | 0.12 |
| LOQ ($\mu g \cdot L^{-1}$) | | 0.17 | 0.23 | 0.40 |

### 3.7. Stability and durability

Stability and durability of the SPME fiber strongly depend on the physicochemical properties and preparation strategy of the coating material, and are important for its practical applications. Generally, the commercially available SPME fibers suffer from swelling in organic solvents.[42] For this reason, the solvent resistance of the HS-$C_8$-S-AgNDs/ESS fibers was investigated after exposure to methanol, chloroform, tetrahydrofuran and dimethylsulfoxide for 36 h, respectively. The fabricated fibers can withstand these organic solvents based on its SEM images. This advantage resulted from the chemical stability of silver and the strong Ag-S bond, and made this fiber suitable for SPME hyphenated with HPLC. Even after 150 extraction (in aqueous phase) and desorption (in mobile phase) cycles, the HS-$C_8$-S-AgNDs/ESS fiber still presented good recovery from 96.3% to 103.0% spiked with 100 $\mu g \cdot L^{-1}$, and three replicates were performed to analyze OD-PABA, EHMC and EHS. Such physical and chemical stability allows the application of this novel fiber for a long time without a significant loss of extraction efficiency. However this fiber has low thermal stability due to its surface functionalization and thereby is used to hyphenate with HPLC in this study.

### 3.8. Analysis of real samples

UV filters are a family of organic compounds with single or multiple aromatic structures, and frequently used in a variety of sunscreens to filter the solar deleterious UV-light that may

cause damage on human skin.[43] These synthetic chemicals has been detected in urban wastewater, e.g. BP-3 and OD-PABA.[44] A critical survey on UV filters determination demonstrated that some UV filters in the aquatic environment possess multiple hormonal activities in vitro.[45] However their concentration is too low to be detected in real water samples with conventional methods. Therefore, the proposed method was employed to preconcentrate and determine UV filters from various environmental water samples. To evaluate the accuracy and precision of the proposed method, recoveries were performed by spiking standard UV filters into the real water samples at concentration levels of 10 μg $L^{-1}$ and 50 μg $L^{-1}$, respectively. The analytical data were listed in Table 2. The relative standard deviation (RSD) was between 5.7% and 8.7% and the mean recoveries ranged from 85.5% to 105.5%.

**Table 2**

**Table 2** Analytical results of UV filters in different environmental water samples (n=3)

| Samples | UV filters | Original (μg $L^{-1}$) | Spiked with 10 μg $L^{-1}$ | | | Spiked with 50 μg $L^{-1}$ | | |
|---|---|---|---|---|---|---|---|---|
| | | | Detected (μg $L^{-1}$) | Recovery (%) | RSD (%) | Detected (μg $L^{-1}$) | Recovery (%) | RSD (%) |
| River water under Bapanxia | OD-PABA | 2.01 | 11.8 | 85.5 | 7.1 | 50.9 | 97.9 | 6.5 |
| | EHMC | 1.82 | 10.9 | 85.7 | 8.3 | 51.2 | 98.8 | 8.6 |

| | | | | | | | | |
|---|---|---|---|---|---|---|---|---|
| Bridge | EHS | ND[a] | 10.2 | 102.0 | 7.6 | 50.5 | 105.5 | 7.9 |
| River water under Yintan Bridge | OD-PABA | 1.22 | 10.7 | 95.3 | 5.8 | 51.0 | 99.6 | 6.4 |
| | EHMC | 0.98 | 10.4 | 94.7 | 7.6 | 50.6 | 99.3 | 8.2 |
| | EHS | ND | 9.8 | 98.0 | 7.2 | 49.2 | 98.4 | 7.4 |
| River water under Donggang Bridge | OD-PABA | 2.89 | 13.1 | 101.6 | 5.7 | 53.0 | 100.2 | 6.2 |
| | EHMC | 2.20 | 12.3 | 100.8 | 8.2 | 52.4 | 100.4 | 8.4 |
| | EHS | ND | 10.2 | 102.0 | 7.2 | 51.1 | 102.2 | 7.6 |
| River water under Shichuan Bridge | OD-PABA | 2.01 | 11.5 | 95.8 | 6.5 | 51.9 | 99.8 | 6.6 |
| | EHMC | 1.87 | 11.2 | 94.4 | 8.4 | 50.7 | 97.7 | 8.5 |
| | EHS | ND | 9.7 | 97.0 | 7.3 | 49.8 | 99.6 | 7.4 |
| Wastewater | OD-PABA | 3.12 | 13.4 | 102.1 | 6.9 | 53.5 | 100.7 | 6.8 |
| | EHMC | 2.88 | 13.0 | 100.9 | 8.7 | 52.9 | 100.0 | 8.4 |
| Snow water | EHS | ND | 10.4 | 104.0 | 7.8 | 50.8 | 101.6 | 7.5 |
| | OD-PABA | 1.02 | 10.7 | 97.1 | 6.4 | 50.9 | 99.7 | 6.7 |
| | EHMC | 0.96 | 10.3 | 94.0 | 8.2 | 50.4 | 98.9 | 8.0 |

| | | | | | | | |
|---|---|---|---|---|---|---|---|
| EHS | ND | 9.6 | 96.0 | 7.4 | 48.8 | 97.6 | 7.6 |

a), Not detected or lower than limits of detection.

Fig. 7 shows typical chromatograms of direct HPLC (Fig. 7a) and SPME-HPLC with the HS-$C_8$-S-Ag/ESS fiber for raw (Fig. 7b) and spiked wastewater (Fig. 7e). The matrix effect was negligible. As compared with commercially available 85 μm PA (Fig. 7c) and 100 μm PDMS (Fig. 7d) fibers, the HS-$C_8$-S-AgNDs/ESS fiber (Fig. 7e) exhibits the greatest extraction capability for target UV filters from spiking wastewater at 50 μg $L^{-1}$. These data demonstrate that the new HS-$C_8$-S-AgNDs/ESS fiber is effective for the preconcentration and determination of trace target UV filters in real environmental water samples.

**Fig. 7**

**Fig. 7.** Typical chromatograms of direct HPLC (a), SPME-HPLC with SH-$C_8$-S-Ag/ESS fiber for raw wastewater (b) and SPME-HPLC with 85 μm PA fiber (c), 100 μm PDMS fiber (d) and SH-$C_8$-S-AgNDs/ESS fiber (e) for spiking wastewater at 50 μg $L^{-1}$.

### 3.9. Comparison of the proposed method with previously reported methods

Up to now, various pretreatment techniques have been used for the concentration and determination of UV filters from water samples, such as SPME-GC,[44] solid phase extraction

(SPE),[46] single-drop microextraction (SDME),[47] hollow fiber supported liquid phase microextraction (HF-LPME)[48] and dispersive liquid-liquid microextraction (DLLME),[49] SPME-HPLC-DAD,[50] SPME-HPLC-UV.[14,51-52] Comparison of the proposed method with previously reported ones was summarized in Table 3 with regard to extraction time (t), linear ranges, RSD, LOD and recovery. The ideal LOD values were obtained. Moreover the HS-$C_8$-S-AgNDs coating permits fast mass transfer from bulky phase to the fiber. The fabricated fiber can be handled with great convenience compared with commercially available polymeric fibers. The operation procedure of SPME-HPLC is a simple and rapid. This novel fiber can selectively preconcnetrate and sensitively determinate target analytes in real environmental water samples. The experimental results for the proposed method are better than those reported in the literatures[14,44,48] and comparable with those reported in the literatures[46-47,49-52].

**Table 3**

**Table 3** Comparison of the current method with previously reported methods for extraction and determination of UV filters.

| Instrumentation[a] | T (min) | Linear ranges ($\mu g \cdot L^{-1}$) | LOD ($\mu g \cdot L^{-1}$) | RSD (%) | Recovery (%) | Ref. |
|---|---|---|---|---|---|---|

| | | | | | | |
|---|---|---|---|---|---|---|
| PDMS-SPME-GC-FID | 45 | 10-500 | 0.87-2.47[b] | 4.5-7.9 | 82-98 | 44 |
| $C_{18}$-SPE-LC-DAD | ~30 | 0.02-0.2 | 0.014[b] | 2.77 | 95-97 | 46 |
| IL-SDME-LC-UV | 37 | 1-150 | 0.07-0.19 | 2.8-7.9 | 96-110 | 47 |
| IL-HF-LPME-HPLC-UV | 50 | 5-1000 | 0.2-0.5 | 1.1-8.4 | 95.2-104.9 | 48 |
| IL-DLLME-HPLC-UV | 10 | 0.5-500 | 0.06-0.16 | 2.8-7.6 | 92.8-114 | 49 |
| PDMS-SPME-HPLC-DAD | 30 | 0.25-100 | 0.06-0.21<br>0.12-0.73 | 3.34-10.21<br>4.23-9.16 | 84.62-100.80<br>81.54-102.32 | 50 |
| $C_{12}$-SPME-HPLC-UV | 60 | 5-200 | 0.69-1.37 | 0.58-1.86 | 69.7-102.4 | 14 |
| Ti–$TiO_2$–$ZrO_2$-SPME-HPLC-UV | 30 | 0.5-400 | 0.038-0.082 | 4.3-12 | 82.2-106.6 | 51 |
| ph-$TiO_2$–Ti-SPME-HPLC-UV | 30 | 0.005-25 | 0.0001-0.05 | 4.6-9.1 | 86.2-105.5 | 52 |
| SH-$C_8$-S-Ag-SPME-HPLC-UV | 40 | 0.3-400 | 0.05-0.12 | 5.8-8.7 | 85.5-105.5 | This method |

[a] $C_{12}$, dodecyl; $C_{18}$ disks; DAD, diode array detection; FID, flame ionization detection; IL, ionic liquid.

[b] Limit of quantification.

## 4. Conclusions

Novel HS-$C_x$-S-AgNDs/ESS fibers were prepared by electrodeposition of AgNDs coating on the ESS wire and subsequent self-assembly of different alkyldithiols. Among the HS-$C_x$-S-AgNDs/ESS fibers, the HS-$C_8$-S-AgNDs/ESS fiber permits best extraction capability and

selectivity for PAHs, UV filters, PCBs and Triclosan. It was more effective than the commercially available PA and PDMS fibers for SPME of target UV filters and employed to extract several UV filters in aqueous solution. Moreover the fabrication of the HS-$C_8$-S-AgNDs coating was easily performed in a highly reproducible manner. This novel fiber integrates the inherent chemical stability of the Ag coating and the mechanical durability of the SS substrate, and can be used over 150 times. Furthermore the Ag coating can react with functional groups like -SH, -$NH_2$. This approach can control the surface property of the fiber and obtain the better extraction performance fiber in the future.

**Acknowledgements**

The authors gratefully acknowledge financial support from the National Natural Science Foundation of China (Grant no. 21265019).

**References**

1 J. Y. Tian, J. Q. Xu, F. Zhu, T. B. Lu, C. Y. Su and G. F. Ouyang, J. Chromatogr. A, 2013, **1300**, 2.

2 F. K. Liu, J. Chromatogr. A, 2009, **1216**, 9034.

3 C. L. Arthur and J. Pawliszyn, Anal. Chem., 1990, **62**, 2145.

4 D. X. Zhang, L. K. Xue, Q. Zhu and X. Z. Du, Anal. Lett., 2013, **46**, 2290.

5 X. Mo, Y. Xu and W. Fan, J. Agri. Food Chem., 2010, **58**, 2462.

6 Q. L. Ma, N. Hamid, A. E. D. Bekhit, J. Robertson and T. F. Law, Microchem. J., 2012, **111**, 16.

7 X. Zhou, X. Li and Z. Zeng, J. Chromatogr. A, 2006, **1104**, 359.

8 W. Liu, L. Zhang, S. Chen, H. Duan, X. Chen, Z. Wei and G. Chen, Anal. Chim. Acta, 2009, **631**, 47.

9 H. X. Liu, L. Liu, Y. Li, X. M. Wang and X. Z. Du, Anal. Lett., 2014, **47**, 1759.

10 J. J. Feng, M. Sun, H. M. Liu, J. B. Li, X. Liu and S.X. Jiang, Anal. Chim. Acta, 2011 **701**, 174.

11 J. H. Fendler, Chem. Mater., 2001, **13**, 3196.

12 H. Bagheri, Z. Ayazi and H. Sistani, Microchim. Acta, 2011, **174**, 295.

13 B. B. Prasad, M. P. Tiwari, R. Madhuri and P. S. Sharma, J. Chromatogr. A, 2010, **1217**, 4255.

14 J. Li, L. Y. Ma, M. Q. Tang and L. Xu, J. Chromatogr. A, 2013,**1298**, 1.

15 J. J. Feng, M. Sun, H. M. Liu, J. B. Li, X. Liu and S. X Jiang, J. Chromatogr. A, 2010, **1217**, 8079.

16 Y. X. Yang, Y. Li, H. X. Liu, X. M. Wang and X. Z. Du, J. Chromatogr. A, 2014, **1372**, 25.

17 Z. Sun, J. H. Kim, Y. Zhao, F. Bijarbooneh, V. Malgras, Y. Lee, Y. M. Kang and S. X. Dou, J. Am. Chem. Soc., 2011, **133**, 19314.

18 A. Mohanty, N. Garg and R. C. Jin, Angew. Chem. Int. Edit., 2010, **49**, 4962.

19 S. Tong, Y. Xu, Z. Zhang and W. Song, J. Phys. Chem. C, 2010, **114**, 20925.

20 T. N. Huan, T. Ganesh, K. S. Kim, S. Kim, S. H. Han and H. Chung, Biosens. Bioelectron, 2011, **27**, 183.

21 L. Wang, W. Mao, D. Ni, J. Di, Y. Wu and Y. Tu, Electrochem. Commun., 2008, **10**, 673.

22 G. W. Lu, C. Li and G. Q. Shi, Chem. Mater., 2007, **19**, 3433.

23 X. L. Tang, P. Jiang, G. L. Ge, M. Tsuji, S. S. Xie and Y. J. Guo, Langmuir, 2008, **24**, 1763.

24 D. Huang, X. Bai and L. Zheng. J. Phys. Chem. C, 2011, **115**, 14641.

25 X. Han, D. Wang, J. Huang, D. Liu and T. You, J. Colloid Interf. Sci., 2011, **354**, 577.

26 Y. Qin, Y. Song, N. J. Sun, N. Zhao, M. X. Li and L. M. Qi, Chem. Mater., 2008, **20**, 3965.

27 J. C. Zhang, L. J. Meng, D. B. Zhao, Z. F. Fei, Q. H. Lu and P. J. Dyson, Langmuir, 2008, **24**, 2699.

28 X. L. Xu, J.B. Jia, X. R. Yang and S. J. Dong, Langmuir, 2010, **26**, 7627.

29 T. Huang, F. Meng and L. Qi, Langmuir, 2010, **26**, 7582.

30 T. H. Lin, C. W. Lin, H. H. Liu, J. T. Sheu and W.H. Hung, Chem. Commun., 2011, **47**, 2044.

31 J. J. Feng, A. Q. Li, Z. Lei and A. J. Wang, ACS Appl. Mater. Interfaces, 2012, **4**, 2570.

32 Z. Y. Lv, A. Q. Li, Y. Fei, Z. Li, J. R. Chen, A. J. Wang and J. J. Feng, Electrochim. Acta, 2013, **109**, 136.

33 A. K. Das, J. Samdani, H. Y. Kim and J. H. Lee, Electrochim. Acta, 2015, **158**, 129.

34 Guide to the Expression of Uncertainty in Measurement, International Organization of Standardization (ISO), Geneva, 1993.

35 P. Konieczka and J. Namie´snik, J. Chromatogr. A, 2010, **1217**, 882.

36 L. E. Vanatta and D.E. Coleman, J. Chromatogr. A, 2007, **1158**, 47.

37 V. J. Barwick, S. L. R. Ellison, C. L. Lucking and M. J. Burn, J. Chromatogr. A, 2001, **918**, 267.

38 H. L. Xu, Y. Li, D. Q. Jiang and X.P. Yan, Anal. Chem., 2009, **81**, 4971.

39 X. Y. Cui, Z. Y. Gu, D. Q. Jiang, Y. Li, H. F. Wang and X. P. Yan, Anal. Chem., 2009, **81**, 9771.

40 N. Chang, Z. Y. Gu, H. F. Wang and X. P. Yan, Anal. Chem., 2011, **83**, 7094.

41 S. Endo, A. Pfennigsdorff and K. Goss, Environ. Sci. Technol., 2012, **46**, 1496.

42 M. D. F. Alpendurada, J. Chromatogr. A, 2000, **889**, 3.

43 A. Salvador and A. Chisvert, Anal. Chim. Acta, 2005, **537**, 1.

44 D. A. Lambropoulou, D. L. Giokas, V. A. Sakkas, T. A. Albanis and M. I. Karayannis, J. Chromatogr. A, 2002, **967**, 243.

45 P. Y. Kunz and K. Fent, Aquat. Toxicol., 2006, **79**, 305.

46 D. L. Giokas, V. A. Sakkas and T. A. Albanis, J. Chromatogr. A, 2004, **1026**, 289.

47 L. Vidal, A. Chisvert, A. Canals and A. Salvador, Talanta, 2010, **81**, 549.

48 D. D. Ge and H. K. Lee, J. Chromatogr. A, 2012, **1229**, 1.

49 L. K. Xue, W. W. Ma, D. X. Zhang and X. Z. Du, Anal. Methods, 2013, **5**, 4213.

50 J. Y. Shen, M. S. Chang, S. H. Yang and G. J. Wu, J. Liq. Chromatogr. Relat. Technol., 2012, **35**, 2280.

51 Y. Li, Y. X. Yang, H. X . Liu, X. M. Wang and X. Z. Du, Anal. Methods, 2014, **6**, 8519.

52 L. Li, R. B. Guo, Y. Li, M. Guo, X. M. Wang and X. Z. Du, Anal. Chim. Acta, 2015, **867**, 38.

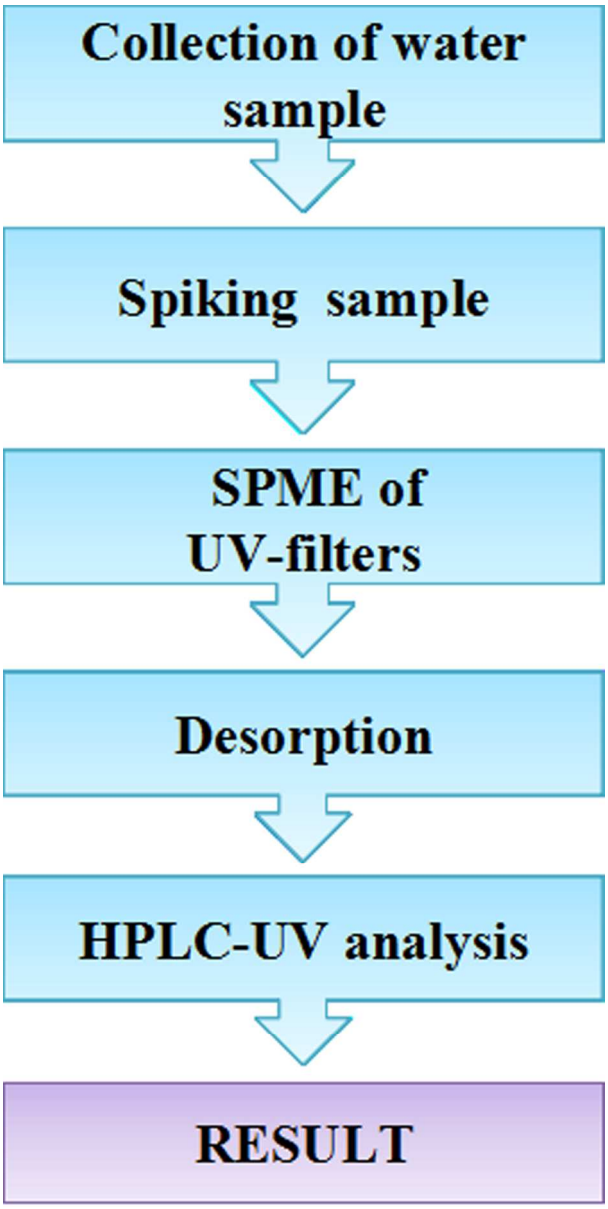


69x139mm (300 x 300 DPI)

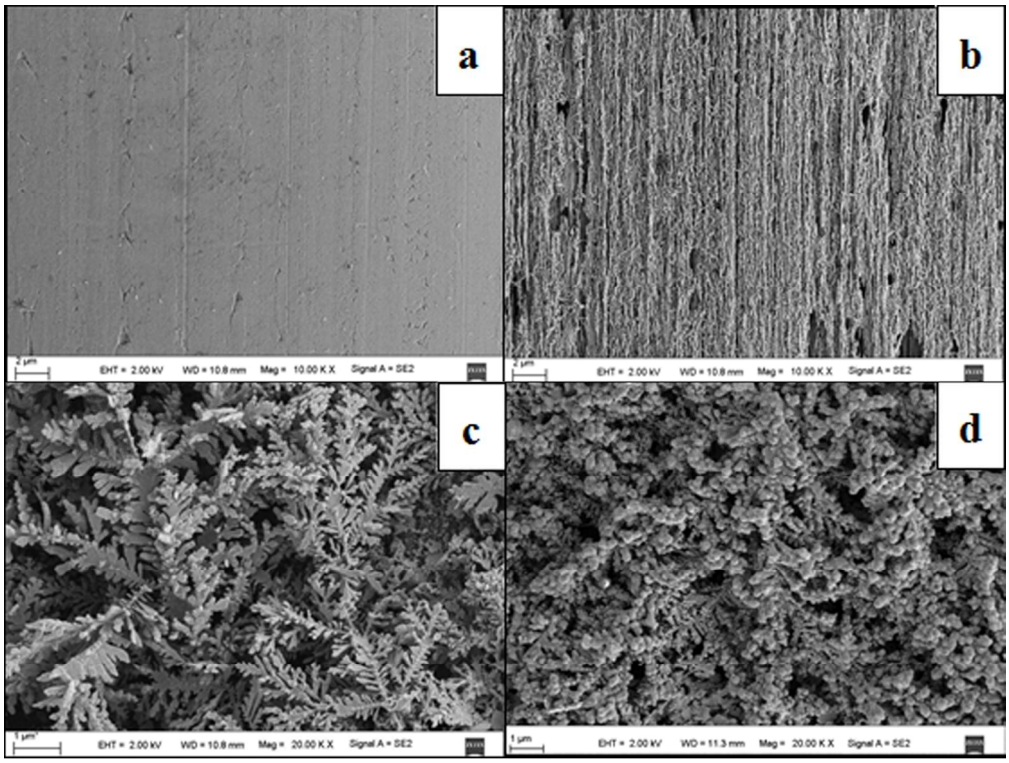


110x83mm (300 x 300 DPI)

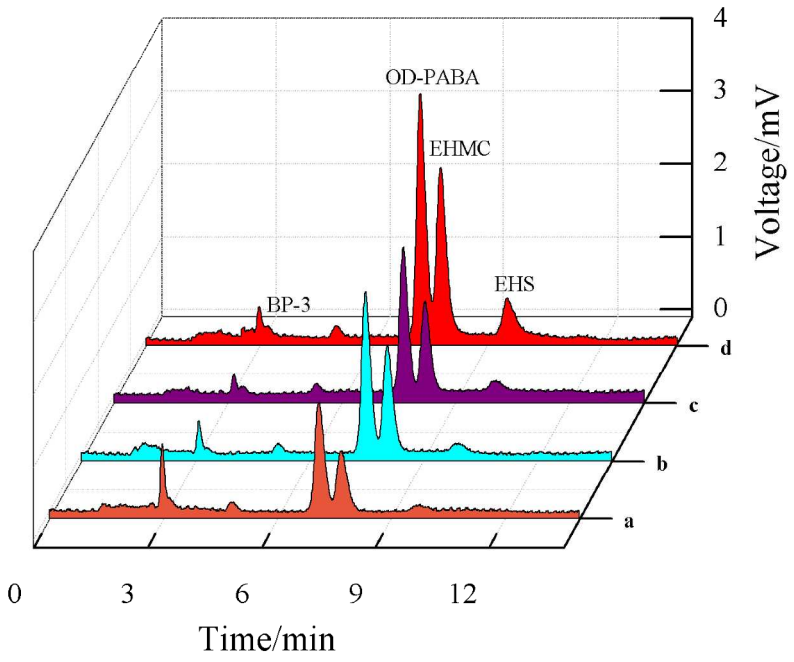


297x209mm (300 x 300 DPI)

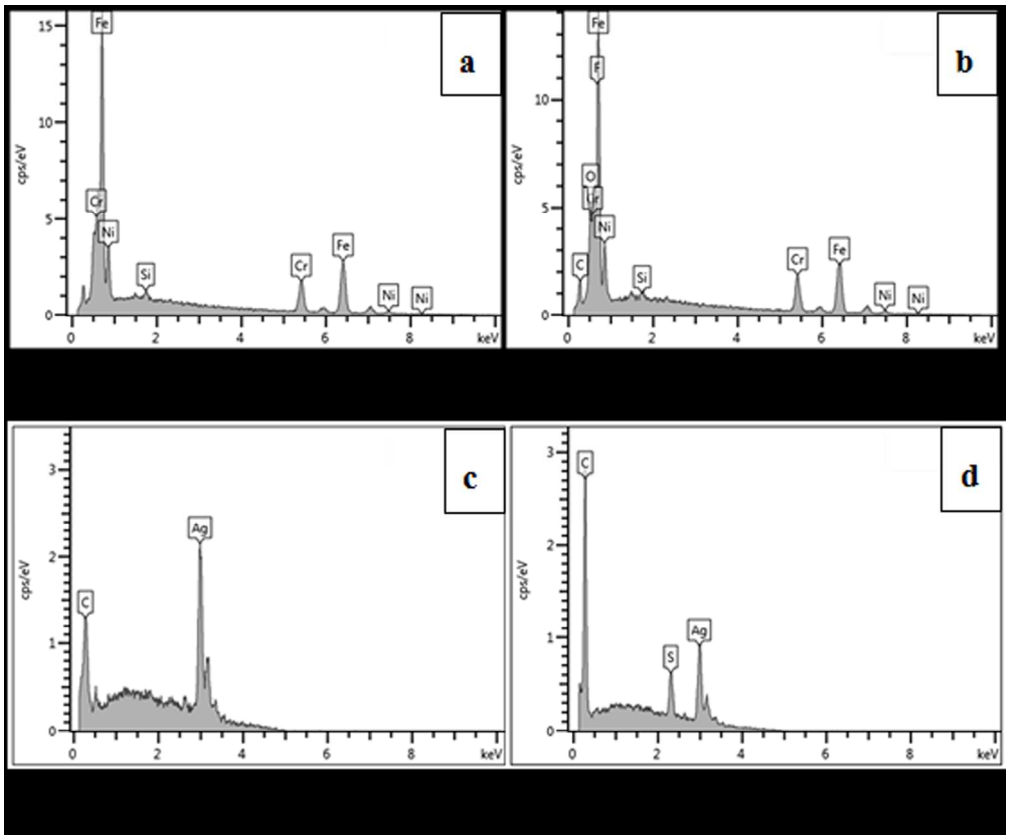


146x121mm (300 x 300 DPI)

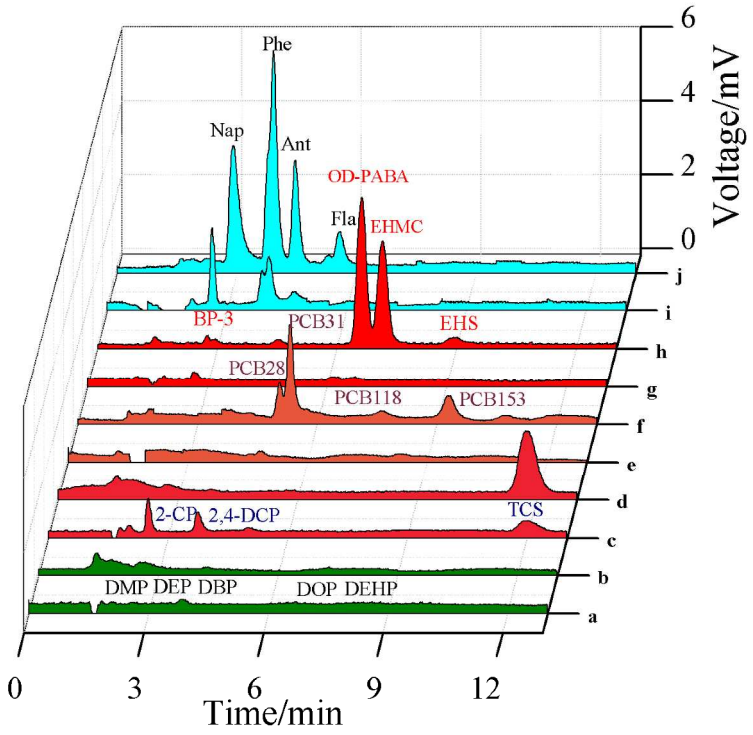


297x229mm (300 x 300 DPI)

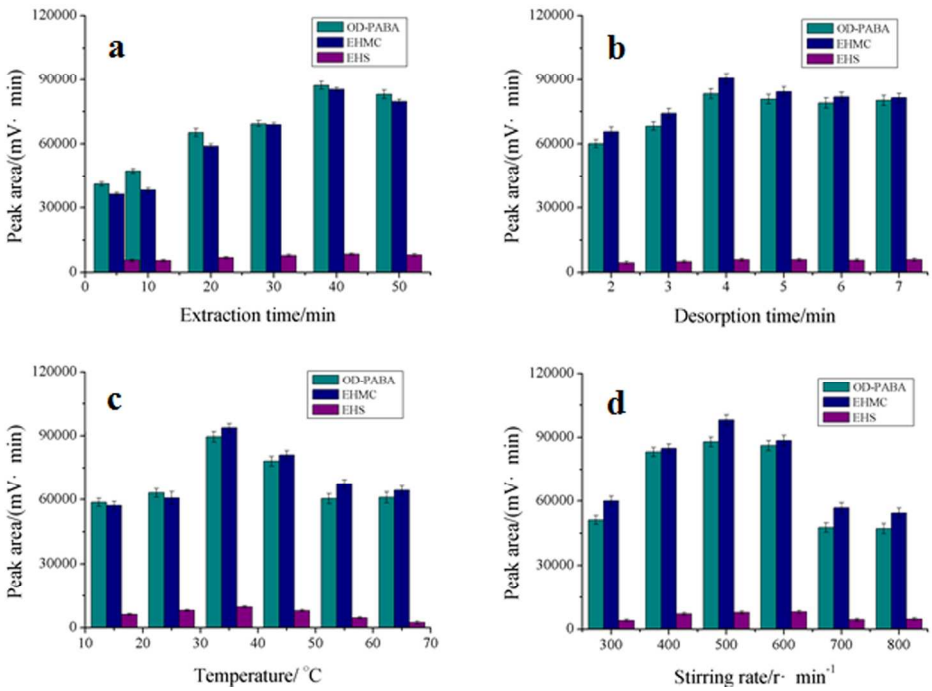


177x126mm (300 x 300 DPI)

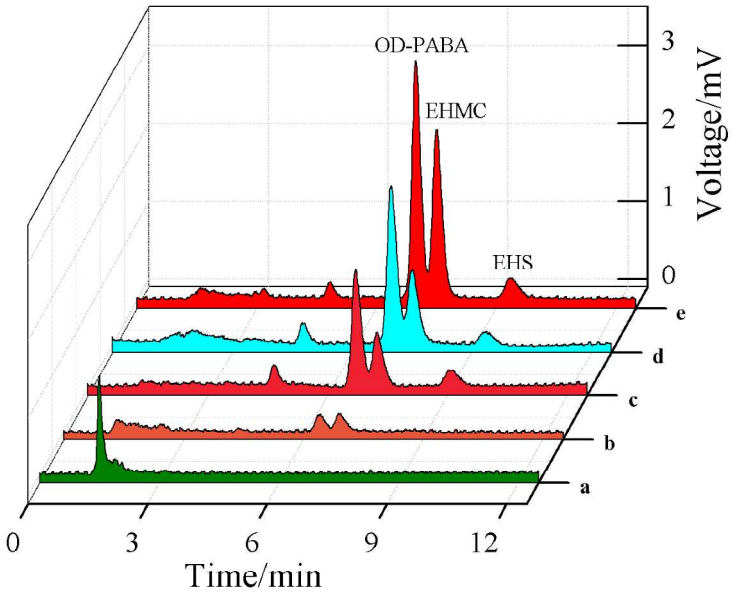


297x209mm (300 x 300 DPI)

**Figure captions**

**Fig. 1.** Flow diagram of the procedure of UV-filters determination in water samples by HPLC-UV method.

**Fig. 2.** SEM images of bare SS wire (a×10000), ESS wire (b×10000), AgNDs coating (c×20000) and SH-$C_8$-S-AgNDs/ESS (d×20000) fibers. Conditions: applied voltage, -0.3 V to 0.3 V; scan rate, 20 mV $s^{-1}$; CV cycles, 20; SAM,12 h; 25□.

**Fig. 3.** Chromatograms of UV filters by SPME-HPLC with the SH-$C_2$-S-AgNDs/ESS (a), SH-$C_3$-S-AgNDs/ESS (b), SH-$C_6$-S-AgNDs/ESS (c) and SH-$C_8$-S-AgNDs/ESS (d) fibers. Conditions: UV filters, 100 μg $L^{-1}$; extraction, 30 min; desorption, 4 min; temperature, 35 $^{o}$C; stirring, 500 r $min^{-1}$.

**Fig. 4.** EDS spectra of bare SS wire (a), ESS wire (b), AgNDs/ESS fiber (c) and SH-$C_8$-S-AgNDs/ESS fiber (d).

**Fig. 5.** Typical chromatograms of direct HPLC for PAEs (a), CPs (c), PCBs (e), UV filters (g) and PAHs (i) as well as corresponding SPME-HPLC with SH-$C_8$-S-AgNDs/ESS fiber for PAEs (b), CPs (d), PCBs (f), UV filters (h) and PAHs (j) for water spiked with 100 μg $L^{-1}$ each analyte.

**Fig. 6.** Dependence of extraction efficiency on extraction time (a), desorption time (b), temperature (c) and stirring rate (d). Error bars are corrected standard deviation of peak areas for three replicates at the 95% confidence level.

**Fig. 7.** Typical chromatograms of direct HPLC (a), SPME-HPLC with SH-$C_8$-S-Ag/ESS fiber for raw wastewater (b) and SPME-HPLC with 85 μm PA fiber (c), 100 μm PDMS fiber

(d) and SH-$C_8$-S-AgNDs/ESS fiber (e) for spiking wastewater at 50 μg $L^{-1}$.

## Graphical Abstract